Cation ordering induced polarization enhancement for PbTiO_{3}-SrTiO_{3} ferroelectric-dielectric superlattices

Junkai Deng, Alex Zunger, and Jefferson Zhe Liu

Phys. Rev. B **91**, 081301 — Published 17 February 2015

DOI: 10.1103/PhysRevB.91.081301

Cation ordering induced polarization enhancement for $PbTiO_3$-$SrTiO_3$ ferroelectric-dielectric superlattices

Junkai Deng,[1] Alex Zunger,[2] and Jefferson Zhe Liu[3,*]

[1] *State Key Laboratory for Mechanical Behavior of Materials, Xi'an Jiaotong University, Xi'an 710049, China*
[2] *University of Colorado, Boulder, Colorado 80309, USA*
[3] *Department of Mechanical and Aerospace Engineering, Monash University, Clayton, Victoria 3800, Australia*

In this paper, an efficient computational material design approach (cluster expansion) is employed for the ferroelectric $PbTiO_3/SrTiO_3$ system. Via exploring a configuration space including over 3×10^6 candidates, two special cation ordered configurations: either perfect or mixed 1/1 (011) superlattice, are identified with the mostly enhanced ferroelectric polarization by up to about 95% in comparison with the (001) superlattice. We find that the exotic couplings between the antiferrodistortive (AFD) and ferroelectric (FE) modes (*e.g.*, AFD_x-FE_z and AFD_{xy}-FE_z), which is absent from the PTO and STO, as the origin for the best polarization property of the two superlattices. This understanding should provide fresh ideas to design multifunctional perovskite heterostructures.

PACS numbers: 77.55.Px, 77.22.Ej, 61.66.Dk,

Searching a large space of superlattice configurations for the one having target properties: Advances in layer-by-layer growth from oxide building blocks $(X)_n/(Y)_m$ [1, 2] now permit laboratory realization of numerous layer sequences (n, m, n', m'...), each having in principle different, configuration-dependent physical properties not normally accessible by the isolated end-point components. However, since the number of possible configurations σ ($\sim 2^N$, possible from a N unit-cells two- component superlattice) far exceeds what could be practically grown exhaustively, the search for the 'magic configuration' σ^* having desired target properties has generally been reduced to sporadic explorations of just a tiny fraction of this astronomic space, often inspecting just a few simple periods (n, m) such as (1,1), (2,2), (2,3) [3]. Here we focus on the computational search of $\sim 3\times10^6$ heterostructure configurations realizable from the X=$PbTiO_3$ and Y=$SrTiO_3$ building blocks that has the maximal ferroelectric polarization P possible in this space. We do so by first calculating via density functional theory (DFT) the polarization $P_{\rm DFT}(\sigma)$ of $\sim$ 50 configurations and using this knowledge to construct a robust cluster expansion (CE) $P_{\rm CE}(\sigma)$ that captures with precision of 3% the polarization $P_{\rm DFT}(\sigma)$ of configurations included as well as excluded from the fit. Since evaluation of $P_{\rm CE}(\sigma)$ for a given σ takes 10^{-5} of the typical effort needed to calculate $P_{\rm DFT}(\sigma)$, this CE can now be searched almost effortlessly for $\sim$ 3,000,000 configurations ($N < 20$), thus readily identifying the magic configurations σ^*= $(PbTiO_3)_1/(SrTiO_3)_1$ and $(Pb_{0.5}Sr_{0.5}TiO_3)_1/(SrTiO_3)_1$ both along the (011) direction as having a [001] polarization value $\sim$ 55% higher than the linear interpolation of the two end point constituents, and $\sim$ 40% higher than the random alloy, and $\sim$ 95% higher than the (001) superlattices. This approach allows us to focus on the analysis of new physical mechanisms directly for the configurations that matter, not for arbitrary configurations that may or may not have new physics. We analyse the physical origins of what makes these best candidates special, finding that the enhancement in ferroelectric polarization originates from a surprising effect previously overlooked in perovskiste heterostructure, *i.e.*, the antiferrodistortive-ferroelectric (AFD_x-FE_z or AFD_{xy}-FE_z) coupling, unique to the superlattice interfaces and absent from the building blocks PTO and STO. This understanding could allow in the future to introduce exotic AFD-FE couplings via heterostructure design for novel multifunctional perovskite materials, *e.g.*, multiferroics [1, 4].

DFT calculation of the polarization: First-principles calculations based on density functional theory (DFT) were performed using the local density approximation [5] and the projector augmented wave method [6] implemented in the Vienna Ab Initio Simulation Package [7]. The use of periodic boundary conditions imposed short-circuit electrical conditions. The in-plane lattice constant was fixed to 3.864 Å to account the constraint from a cubic STO substrate. All ionic positions were relaxed until the forces were less than 5 meV/Å. Due to a small lattice mismatch of STO and PTO ($< 0.05\%$), the constraint effects on P and total energy are insignificant. The electric polarization was computed by using the bulk Born effective charges [8], *i.e.*, $Z^*_{\rm Pb,Sr} = 2.7$ and $Z^*_{\rm Ti} = 4.6$ and the cation off-centre displacement of fully relaxed configuration in DFT calculations. The selected values of bulk Born effective charges yielded an excellent agreement with results using the Berry phase method [8].

Constructing an expansion for polarization as a function of configuration: The CE approach [9, 10] can map the relations between different configurations and their physical properties. For a binary mixture, one defines a configuration σ as a specific decoration of two types of

building-units on a given Bravais lattice, in which each lattice site is occupied by either of the two (spin variable $s_i = -1$ or $= 1$, respectively). The property of interest $\mathcal{F}$ can then be expressed as:

$$\mathcal{F}_{\rm CE}(\sigma) = J_0 + \frac{1}{N}[\sum_i J_i s_i + \sum_{i,j} J_{ij} s_i s_j + \sum_{i,j,k} J_{ijk} s_i s_j s_k + \cdots] \quad (1)$$

where J_{ij}, J_{ijk}, $\cdots$ represent the effective-cluster interactions (ECIs) for pair, three-body, $\cdots$, interactions in the chemical system, and the $s_i s_j$, $s_i s_j s_k$, $\cdots$ are the multisite cluster functions that form a complete basis set in the configuration space. The ECIs can be obtained by fitting the first-principles calculated results ($\mathcal{F}$) of a set of ordered configurations to Eq. (1). The CE approach has been applied to total energy[9], Curie temperature [11], elastic modulus [12], thermo-conductivity [13]) and so on. It is applied here for the first time to ferroelectric polarization.

Using the data from DFT calculations, an iterative training process was used to fit the ECIs in Eq. (1) [14]. A good convergence was achieved with only 48 DFT inputs. The obtained $P_{\rm CE}(\sigma)$ includes 15 pairs, 1 triplet, 3 quadruplet, and 1 quintuplet clusters. The cross-validation score [15], representing the prediction error of $P_{\rm CE}(\sigma)$, is less than 0.011 C/m^2.

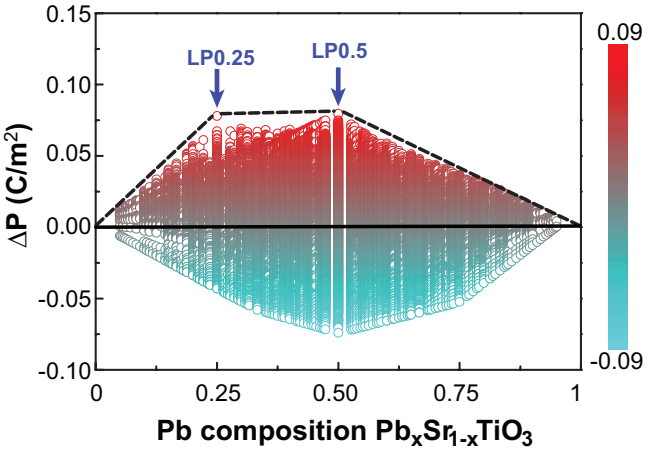

FIG. 1. Polarization enhancement of PTO/STO configurations with respect to the concentration weighted average of bulk PTO and STO, $\Delta P_{\rm CE}(\sigma)$, predicted by the cluster expansion approach. The two configurations at breaking points of the convex hull represent the optimal configurations with the largest polarization (LP) at PTO concentration of 0.25 and 0.5 (named LP0.25 and LP0.5), respectively.

Searching ∼3,000,000 configurations for Identifying the one with the largest polarization: Fig. 1 and Fig. S1 show the polarization enhancement $\Delta P_{\rm CE}(\sigma)$ of the O(3×10^6) ordered configurations with respect to the concentration weighted average of the bulk PTO and STO. The two breaking points of the convex hull (PTO concentration of 0.25 and 0.5) represent the configurations of the largest polarization (LP) that exhibit the mostly enhanced P values. Their crystal structures are presented in Fig. 3 and Fig. S2. Their P values are 0.237 C/m^2 and 0.392 C/m^2, *i.e.*, an enhancement of 95%, and 71% in comparison with the counterpart (001) SLs, respectively (Fig. S1) [16].

Careful inspection reveals a common cation ordering motif in Fig. 3 and Fig. S2. The LP0.5 is a perfect $(PbTiO_3)_1/(SrTiO_3)_1$ (011) SL. The LP0.25 is an intermixed $(Pb_{0.5}Sr_{0.5}TiO_3)_1/(SrTiO_3)_1$ (011) SL. Such special configurations were not expected before but successfully identified by CE. Note that the two LP configurations have a lower total energy than the (001) SL counterparts and other heterostructures (Table SIII) [16], suggesting that they should be feasible experimentally. In addition, experimental methods to grow short period (011) pervoskite SLs were already demostrated [17]. Since the short period structures explored here are expected to remain coherent, they would also be well within the currently available growth capabilities; their growth is thus called for.

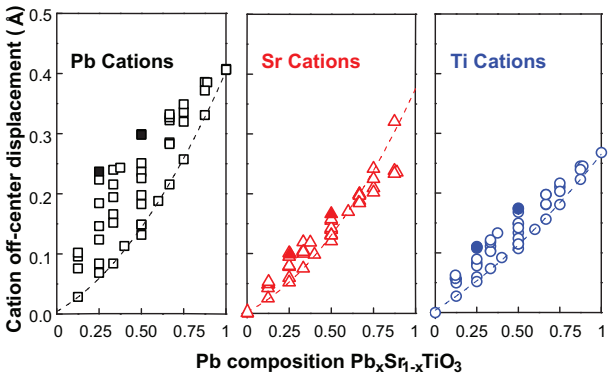

FIG. 2. Average off-center displacements of (a) Pb, (b) Sr and (c) Ti cations of the DFT calculated 48 configurations. The dashed lines are fitted to off-center displacements of the (001) superlattices.

The mechanism leading to maximal polarization – AFD-FE coupling in the LP configurations: The roles of different cations in determining the FE polarization can be seen in Fig. 2, where averaged cation off-centre displacements of the 48 configurations calculated using DFT are summarised. The dashed lines in Fig. 2 depict results for the (001) PTO/STO superlattices. The solid symbols represent results for those two LP configurations (Fig. 1), indicating the largest cation off-centre displacements (thus the largest FE polarization). A much less variation of the averaged Sr and Ti off-centre displacements among configurations suggests the primary role of the Pb cations.

To elucidate origin of the enhanced polarization of the LP configurations, the relaxed crystal structures of LP0.5 and LP0.25 (Fig. 3) are carefully examined using the symmetry mode analysis program ISOTROPY suite [18].

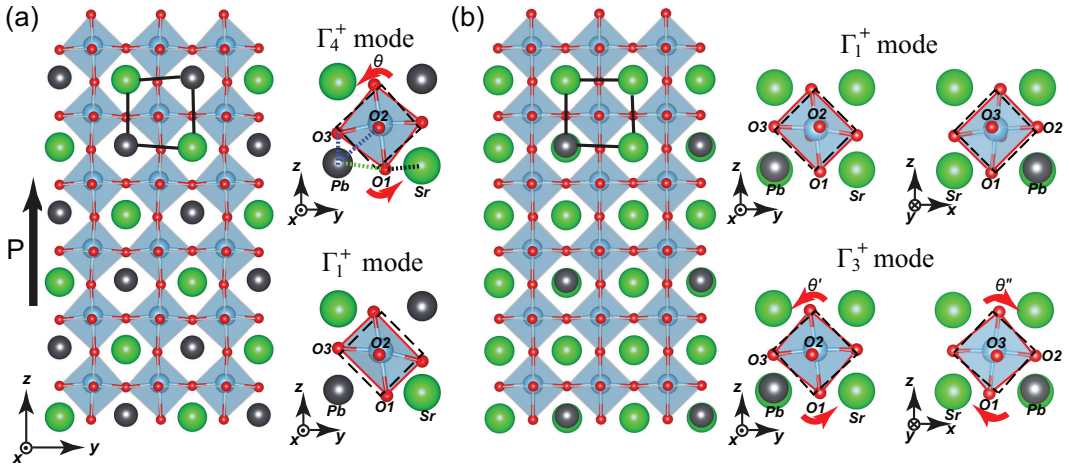

FIG. 3. Relaxed structures and two primary AFD modes of the (a) LP0.5 and (b) LP0.25 in DFT calculations. In LP0.5, the primary mode Γ_4^+ represents an octahedra tilting along x axis with oxygen atom in (001) plane moving toward Sr cations (the Glazer notation $a^+b^0b^0$). The secondary Γ_1^+ mode represents a shape distortion of octahedra with oxygen atoms O_1 and O_3 moving toward Sr cations. Interestingly the two primary modes of LP0.25, Γ_1^+ and Γ_3^+ (Glazer notation $a^+a^+c^0$), resemble those of LP0.5. See text for details.

The results are summarised in Fig. 3, Table I and Table SI [16]. Two primary AFD distortion modes of the LP0.5 are shown in Fig. 3(a). The Γ_4^+ mode represents a tilting of octahedra about x axis with a titling angle of $\theta = 2.9^o$, consequently in (001) plane the oxygen atoms moving away from the Pb and toward the Sr cations. The Γ_1^+ mode represents a shape distortion of octahedra, *i.e.*, the Ti-O bonds being bent toward the Sr cations in the yz plane. It is interesting to note that the two primary AFD modes of the LP0.25 [Fig. 3(b)], Γ_1^+ and Γ_3^+, resemble those of LP0.5, except that in mode Γ_1^+ the Ti-O bonds are bent in both the xz and yz planes and the octahedra tilting in Γ_3^+ mode takes place along both x and y axis.

To examine the coupling between the AFD and the FE modes, we artificially 'turn off' these AFD modes in the LP structures meanwhile allowing the FE polarization to fully develop in DFT calculations. The results are shown in Table I. Turning-off the minor distortion modes ('others' in Table I and Table SI) in LP0.5 slightly enhance the P to 0.396 C/m^2. It suggests that these AFD distortion modes indeed suppress the FE polarization, consistent with the traditional views in perovskites. In contrast, Γ_4^+ and Γ_1^+ modes promote the polarization, turning-off of these two modes significantly reducing the polarization value down to 0.354 C/m^2 together with an increase of total energy. The same conclusion can be drawn for LP0.25, *i.e.*, the AFD modes enhancing the P values monotonously from 0.209 to 0.237C/m^2. For the PTO/STO 1/1 or 2/2 (001) SLs, the out-of-plane AFD$_z$-FE$_z$ coupling [4] and the in-plane AFD$_{xy}$-FE$_{xy}$ coupling [19] have been observed. The discovered coupling between in-plane AFD$_x$ or AFD$_{xy}$ (*i.e.*, Γ_4^+ in LP0.5 and Γ_3^+ in LP0.25) and out-of-plane FE$_z$ modes in our LP structures has not been reported. Interestingly, these distortion modes and their couplings do not exist in the parent constituents, either. This observation gives us an important clue that *new distortion modes and their couplings can be introduced via designing the heterostructures.*

Note that the LP configurations can be seen as intermixed (001) SLs (Fig. 3 and Fig. S2). It was proposed that by introducing some degree of interface cation mixing to a ferroelectric-dielectric superlattice could enhance FE polarization [8]. This is because to avoid the electrostatic energy penalty from the net charge accumulated at interfaces, the FE/dielectric layer will be depolarized/polarized to yield similar polarization values, often leading to a reduced total polarization value [4, 8]. Introducing interlayer cation mixing could reduce the energy penalty and thus enhance the polarization P. In Table I, the intermixing effect of LP0.5 indeed reduces the total energy and increases the polarization significantly in comparison with the (001) SL, apparently supporting the model from Cooper et al. [8]. But an exception is observed for LP0.25. The intermixing does not reduce the total energy, whereas it significantly enhances the P value. Appearently there is no simple model to account for the interface mixing effect on FE polarization.

The AFD-FE coupling plays a decisive role in determining the LP structures. Our DFT calculations show that a Sr cation dopant in $PbTiO_3$ tends to attract oxygen atoms moving toward it (Fig. S4) [16, 19]. For the LP0.5, the check-board cation ordering pattern in the yz plane [Fig. 3(a) and Fig. S2] ensures the two Sr cations (neighbouring a Pb cation) can work collaboratively to maximise the Γ_4^+ and Γ_1^+ modes. In the LP0.25, the Pb cations show a BCC ordered pattern on the simple cubic Bravis lattice (Fig. S2), in which all 6 nearest neighbours of every Pb cation are the Sr cations. These Sr

neighbours should work collaboratively to maximise the Γ_1^+ and Γ_4^+ modes. Structural analysis indicates that the LP0.5 and LP0.25 have the largest octahedra titling angle and Ti-O-Ti bending angle among all the configurations studied in our DFT calculations at $x = 0.25$ and 0.50 (Fig. S5 and Table SIII), respectively. For a comparison, we noticed one specific structure str381 (Fig. S6), which has a very similar cation ordered pattern as LP0.5. If only considering the intermixing effect, the str381 has a lower total energy and a higher P value than those of LP0.5 (Table SIV). But the small variation in ordered pattern results in a weaker collaborative effect, leading to a smaller tilting angle and Ti-O bending angle in str381 (Table SIII). The AFD-FE coupling thus yields a larger P increase for the LP0.5 to overtake str381 as the LP configuration at $x = 0.5$ (Table SIV). We believe that the AFD$_x$-FE$_z$ or AFD$_{xy}$-FE$_z$ coupling is the origin for LP structures to have the largest polarization enhancement among the 3×10^6 candidates. Interesting, such unexpected coupling leads to the best FE polarization.

Physical origins for the AFD$_x$-FE$_z$ coupling: Figure 4 shows the difference-electron density analysis and the projected partial density of states (pDOS) for Pb and its neighbouring O ions in the LP0.5 (without/with AFD$_x$). Clearly, the octahedra titling can significantly enhance the hybridisation between the Pb 6s and the O 2p orbitals, evidenced by the strongly overlapped peaks in pDOS and the strong charge redistribution among the Pb and O ions. For bulk PTO, it is well established that the hybridisation between the Pb lone pair 6s electrons and the O 2p electrons induces its superior FE properties. The enhanced electronic hybridisation caused by the AFD$_x$ titling is, therefore, origin for the observed increase of FE$_z$ polarization [19].

The importance of AFD-FE coupling has been recognised recently for designing multifunctional perovskite heterostructures, because the buckling of the inter-

TABLE I. FE polarization and relative total energy results of the LP0.5 and LP0.25 with the distortion modes subsequently turning-off. A comparison is made with the perfect (001) SLs. In all the cases, the polarization is allowed to fully develop in DFT calculations.

	modes	P$_z$ (C/m^2)	ΔE_{rel} (meV/cell)
LP0.5	Γ_4^+ & Γ_1^+ & Other	0.392	-15.36
	Γ_4^+ & Γ_1^+	0.396	-15.11
	Γ_4^+	0.381	-5.33
	intermixing	0.354	-3.65
(001) 1/1 SL		0.229	0.0
LP0.25	Γ_1^+ & Γ_3^+ & Other	0.237	-4.0
	Γ_1^+ & Γ_3^+	0.232	-3.95
	Γ_1^+	0.224	-3.54
	intermixing	0.209	2.5
(001) 1/3 SL		0.122	0.0

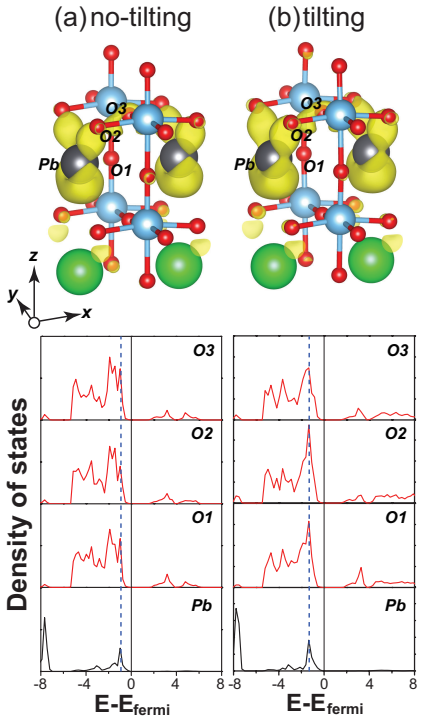

FIG. 4. Difference-electron density and partial DOS for Pb and neighboring O ions in LP0.5 without octahedral tilts (a) and with titling (b). The yellow iso-surfaces are plotted at 0.0045 e^-/bohr^3. In partial DOS results, black lines represent Pb 6s states and red lines represent O 2p states.

octahedra B-O-B bond angles, a direct consequence of the octahedra rotation, can change physical properties, *e.g.*, electronic bandwidth, magnetic interactions, and critical transition temperatures etc [20]. Some elegant design criteria have been proposed, but only considering a limited number of configurations such as the 1/1 and 2/2 (001) SLs etc.[4, 19, 21–25]. In addition, those design rules adopt 'interpolation' of the end-point components to study the SLs. In contrast, our studies show that heterostructures can have unique distortion modes and couplings that are absent from two end-point components, indicating unexplored rich and novel physics in pervoskite systems. Our CE method can serve as a general and efficient means for discoveries and hence to help develop comprehensive design rules.

In summary, an efficient CE approach was used to study the cation ordering effects on the FE polarization in PTO/STO perovskite. Two (011) superlattices are identified as the configurations with the best polarization property. The exotic AFD-FE couplings (the in-plane AFD$_x$ or AFD$_{xy}$ modes and out-of-plane polarization FE$_z$), unique to the SLs and not observed in neither PTO nor STO, are revealed as the origin for the best polarization P. This understanding provides fresh ideas in design of other lone-pair driven ferroelectricity systems, exemplified by $BiFeO_3$ which is the most common mech-

anism to achieve the multiferroics in perovskite [1].

JD and JZL acknowledge the financial support from Monash University Engineering faculty 2013 seed grant. JD also thanks the support of NSFC (51320105014, 51471126), China Postdoctoral Science Foundation (2014M552435) and the Fundamental Research funds for the Central Universities. Work of AZ was funded by DOE, office of science, Basic energy science. The authors gratefully acknowledge computational support from Monash University Sun Grid and the National Computing Infrastructure funded by the Australian Government.

* zhe.liu@monash.edu

[1] R. Ramesh and N. A. Spaldin, Nat Mater. **6**, 21 (2007).
[2] J. C. Jiang, X. Q. Pan, W. Tian, C. D. Theis, and D. G. Schlom, Applied Physics Letters **74**, 2851 (1999).
[3] M. Dawber, C. Lichtensteiger, M. Cantoni, M. Veithen, P. Ghosez, K. Johnston, K. M. Rabe, and J. M. Triscone, Phys. Rev. Lett. **95**, 177601 (2005).
[4] E. Bousquet, M. Dawber, N. Stucki, C. Lichtensteiger, P. Hermet, S. Gariglio, J.-M. Triscone, and P. Ghosez, Nature **452**, 732 (2008).
[5] J. P. Perdew and A. Zunger, Phys. Rev. B **23**, 5048 (1981).
[6] P. E. Blöchl, Phys. Rev. B **50**, 17953 (1994).
[7] G. Kresse and J. Furthmüller, Phys. Rev. B **54**, 11169 (1996).
[8] V. R. Cooper, K. Johnston, and K. M. Rabe, Phys. Rev. B **76**, 020103 (2007).
[9] D. D. Fontaine, Solid State Phys. **47**, 33 (1994).
[10] D. B. Laks, L. G. Ferreira, S. Froyen, and A. Zunger, Phys. Rev. B **46**, 12587 (1992).
[11] A. Franceschetti, S. V. Dudiy, S. V. Barabash, A. Zunger, J. Xu, and M. van Schilfgaarde, Phys. Rev. Lett. **97**, 047202 (2006).
[12] J. Z. Liu, A. van de Walle, G. Ghosh, and M. Asta, Phys. Rev. B **72**, 144109 (2005).
[13] M. K. Y. Chan, J. Reed, D. Donadio, T. Mueller, Y. S. Meng, G. Galli, and G. Ceder, Phys. Rev. B **81**, 174303 (2010).
[14] We started with feeding the $P_{\mathrm{DFT}}(\sigma)$ results of 23 usual suspects to fit the ECIs. Using the obtained $P_{\mathrm{CE}}(\sigma)$, an exhaustive enumeration method was employed to search a configurational space ($\mathrm{O}(3\times10^6)$ configurations) for the largest polarization (LP) configurations. The P_{DFT} results of these LP candidates, if not available, were then determined using DFT calculations and compared against the CE predictions. In the next iteration, these P_{DFT} results were added to the DFT data pool to refit the ECIs, and then the obtained $P_{\mathrm{CE}}(\sigma)$ was used to search for the new LP candidates. This iterative process was repeated until the CE predicted results agreed with the DFT calculations and no new LP configurations were predicted.
[15] A. van de Walle and G. Ceder, J. Phase Equilib. **23**, 348 (2002).
[16] See Supplemental Material at [URL will be inserted by publisher] for total energy and FE polarization results of the PTO/STO heterostructrues using DFT calculations, the AFD-FE coupling analysis, and some insights obtained from analyzing the LP configurations.
[17] A. Annadi, Q. Zhang, X. Renshaw Wang, N. Tuzla, K. Gopinadhan, W. M. L, A. Roy Barman, Z. Q. Liu, A. Srivastava, S. Saha, Y. L. Zhao, S. W. Zeng, S. Dhar, E. Olsson, B. Gu, S. Yunoki, S. Maekawa, H. Hilgenkamp, T. Venkatesan, and Ariando, Nat. Commun. **4**, 1838 (2013).
[18] B. J. Campbell, H. T. Stokes, D. E. Tanner, and D. M. Hatch, J. Appl. Crystallogr. **39**, 607 (2006).
[19] P. Aguado-Puente, P. García-Fernández, and J. Junquera, Phys. Rev. Lett. **107**, 217601 (2011).
[20] M. Imada, A. Fujimori, and Y. Tokura, Rev. Mod. Phys. **70**, 1039 (1998).
[21] X. Wu, K. M. Rabe, and D. Vanderbilt, Phys. Rev. B **83**, 020104 (2011).
[22] J. M. Rondinelli and C. J. Fennie, Adv. Mater. **24**, 1961 (2012).
[23] J. M. Rondinelli, S. J. May, and J. W. Freeland, MRS Bull. **37**, 261 (2012).
[24] J. M. Rondinelli and N. A. Spaldin, Adv. Mater. **23**, 3363 (2011).
[25] A. T. Mulder, N. A. Benedek, J. M. Rondinelli, and C. J. Fennie, Adv. Funct. Mater. (2013).